PRINT-93-0331 (MINNESOTA)
1992
15
Fermilab Library
0 1160 0010444 2

Nuclear and Medium Effects for Hadron Production in Ultra-relativistic Heavy Ion Collisions

Klaus Geiger

School of Physics and Astronomy

University of Minnesota, Minneapolis, MN 55455

Abstract

Properties of hadron production and the charged particle spectra in heavy ion collisions are calculated for the case of central $Au + Au$ collisions at the collider energies of RHIC ($\sqrt{s} = 200$ A GeV) and LHC ($\sqrt{s} = 6300$ A GeV), using a parton cascade / cluster hadronization model. The influence of nuclear shadowing, parton fusion and absorption processes, the Landau-Pomeranchuk effect and the phenomenon of soft gluon interference on the inclusive hadron production is analyzed. Predictions for charged particle spectra and multiplicities are given. In particular, the model results for the central rapidity densities of charged particles are $\simeq 1200$ ($\sqrt{s} = 200$ A GeV) and $\simeq 2500$ ($\sqrt{s} = 6300$ A GeV), which is a factor of ~ 2.5 per nucleon larger than in $p + p$ collisions at corresponding energies.

PACS indices: 12.38.Mh, 25.75.+r, 24.85.+p, 13.87.Fh

ROUTE TO
NAME | LOCATION
KAPOOR 221
RETURN TO

Ultra-relativistic heavy ion collisions ($\sqrt{s} \geq 200$ A GeV) are expected to exhibit new physics effects that are not significant at lower energies or in small sized systems as e.g. hadron-hadron collisions. Of particular interest are phenomena associated with the microscopic dynamics of the partons during these reactions, since they offer to study QCD in hot, ultra-dense nuclear matter and may signal some evidence for the predicted QCD phase transition to a quark-gluon plasma [1]. In this letter I would like to emphasize the impact of a number of nuclear and medium effects on the kinetic evolution of the partons that should be reflected in the inclusive hadron production of heavy ion collisions at the BNL Relativistic Heavy Ion Collider (RHIC) ($\sqrt{s} = 200$ A GeV) and the CERN Lepton Hadron Collider (LHC) ($\sqrt{s} = 6300$ A GeV). A related analysis has recently been carried out by Wang and Gyulassy [2,3] who investigated two such effects in $Au + Au$ collisions at RHIC, namely nuclear shadowing and jet quenching, within a perturbative QCD approach involving multiple minijet production [2]. Connecting to this work, I will adress here the following phenomena with respect to their relevance for multiparticle production in heavy ion collisions:

(i) Nuclear shadowing [4], which is the depletion of soft partons in the nuclear structure functions relative to the ones of a free nucleon, clearly affects the initial parton distributions of the colliding nuclei and therefore should influence the initial conditions of the reactions. This shadowing of partons is evident in the measurements of the nuclear quark structure functions in deep inelastic scattering by the European Muon Collaboration [5] and is expected to be also true for the gluon structure functions [6].

(ii) Parton fusion and absorption processes during the early stage of the nuclear collisions have been shown [7] to substantially supress the emission of gluons through QCD bremsstrahlung. As the phase-space density of partons becomes large in the central collision region, due to intense parton production, the probability for fusion and absorption of partons increases relative to the emission probability and the competing emission and absorption processes tend to a detailed balance.

(iii) The Landau-Pomeranchuk effect [8] associated with multiple frequent scat-

terings of partons in the dense quark-gluon matter of the central region leads also to a suppression of gluon radiation [7]. The radiation emitted by a virtual parton has a characteristic formation time. If such a parton undergoes sucessive scatterings within short times, then the radiation with comparably long formation time cannot be irreversibly be formed but will be suppressed, because the parton has a large probability to rescatter before it can emit a radiative gluon.

(iv) Soft gluon interference [9], known as the destructive interference of gluon emission amplitudes in parton cascades, reduces the multiplicity of gluons produced through QCD bremsstrahlung. It especially affects the soft emission region in which the partons have small momenta and is therefore of particular importance if the number of low energy partons becomes large, as is expected to be the case in heavy ion collisions [7].

The model framework for the analysis is provided by the parton cascade model [7,10] which recently has been supplemented by a suitable phenomenological hadronization scheme [11]. In the parton cascade model ultra-relativistic nuclear collisions are decribed as the time evolution of the parton phase-space distributions. The space-time development is formulated within renormalization group improved QCD perturbation theory, embedded in the framework of relativistic transport theory. The dynamics of the dissipative processes during the early stage of the nuclear reactions is simulated as the evolution of multiple internetted parton cascades associated with quark and gluon interactions. At the end of the perturbative QCD phase the hadronization is modelled as a recombination of the final state partons to form color singlet clusters, followed by the fragmentation ('decay') of these clusters into observable hadronic states. It was demonstrated in Ref. [11] that the parton cascade model combined with this cluster hadronization scheme sets a consistent framework to simulate and study the time evolution of hadron-hadron and nucleus-nucleus collisions in complete phase-space, from the first instant of collision to the final particle yield.

In Ref. [7] it has been investigated how the effects (ii)-(iv) (nuclear shadowing (i) was not considered there) affect the space-time evolution of the system of

partons during the nuclear collisions. It was concluded that these effects lead to a substantially longer duration of the partonic phase before non-perturbative mechanisms become relevant, and to a considerable reduction of the multiplicities of produced gluons and quarks. In the following, the central objective is the question, how clearly the effects (i)-(iv) are reflected in the final hadron spectra and if is it possible to disentangle the significance of the different phenomena. I will therefore consider five different evolution scenarios for the parton distributions, for each of which I have performed simulations of central $Au + Au$ collisions at the collider energies of RHIC and LHC. As shown below, not only give the calculations rather distinct results, but also exhibit a clear impact of nuclear effects in the charged particle spectra when compared with pp collisions at corresponding energies. The evolution schemes are as follows (see Refs. [7,11] for details):

a) *'Naive evolution'*: Parton shadowing in the initial parton distributions is neglected. Parton scatterings occur instantaneously without time delay. Associated cascades of sucessive parton branchings happen immediately at the same space-time point as the scattering, i.e. with zero formation time for radiative emissions. Absorptive processes and soft gluon interference are switched off.

b) *Nuclear shadowing*: As a), but now the initial parton distributions are modified to account for nuclear shadowing effects as explained in Sec. 2.1.

c) *Parton fusion and absorption*: As b), but in addition the time scale for each individual parton-parton collision is taken into account. Parton fusion and absorptive processes compete with the emission of partons in the cascades.

d) *Landau-Pomeranchuk effect*: As c), but furthermore, sucessive parton branchings in the cascade evolution are delayed according to the characteristic formation time for gluon emissions.

e) *Soft gluon interference*: As d), but moreover, the destructive interference of soft gluons decreases the available phase-space for low energetic gluon bremsstrahlung.

To illustrate the new physics associated with the effects in a) - e), I will focus here on the two simplest observables: the pseudorapidity and the transverse momentum

spectra of final charged hadrons. The Figs. 1 and 2 show the charged particle distributions in η, respectively $p_\perp$, calculated for central $Au + Au$ collisions with $\sqrt{s} = 200$ A GeV and $\sqrt{s} = 6300$ A GeV. The various curves a) - e) display the characteristics of the different evolution scenarios. As can be seen from Fig. 1, the particle density in the central rapidity region is reduced sucessively from the 'naive' calculation (case a) to the default result (case e) by more than a factor of 3. For both collider energies the behaviour is roughly the same, although the impact of nuclear shadowing (curve b) and the Landau-Pomeranchuk effect (curve d) seem to become more prominent at $\sqrt{s} = 6300$ A GeV. Obviously the drastic reduction of the charged particle yield is most significant at $\eta \approx 0$, because the inclusion of delayed gluon emission associated with the Landau-Pomeranchuk effect (case d) and soft gluon interference (case e) leads to a specific depletion of softer partons which is reflected by the dip appearing in the range $|\eta| \leq 1$. Although clearly mirrowed in the hadron distributions, both these effects originate from the parton level: First, soft gluon radiation takes a longer formation time than the emission of harder gluons, so that it is suppressed by subsequent parton scatterings before it actually can occur. Second, the destructive interference of soft gluon emission amplitudes yields a further suppression of low energy quanta. The latter effect is a general property of QCD [9], independent of the reaction, and is claimed to be observable also in e.g. $e^+e^- \rightarrow$ hadrons or $p\bar{p}$ $(pp) \rightarrow$ hadrons [12]. On the other hand, the Landau-Pomeranchuk effect associated with the finite formation time of gluon radiation is certainly a novel nuclear phenomenon which not visible in e.g. pp collisions, because there the phase-space density of partons is too low. For the total integrated charged particle yield the reduction from a) to e) is less dramatic than for the central rapidity density, but is still very large: from $\simeq 17000$ to $\simeq 6600$ ($\sqrt{s} = 200$ A GeV) and from $\simeq 42500$ to $\simeq 21500$ ($\sqrt{s} = 6300$ A GeV).

Comparing the η-spectra for RHIC (Fig. 1 a) and LHC (Fig. 1 b) one sees that the central density only doubles (from $\simeq 1200$ to $\simeq 2500$ in case e) when the collider energy is increased by about a factor of 30. However, the total charged multiplicity grows from $\simeq 6600$ to $\simeq 21500$ from RHIC to LHS, i.e. by more than a factor of 3, because not only the height but also the width of the spectra increases.

At this point it is of interest to note that the results obtained here for the charged central rapidity densities are in qualitative agreement with the estimates obtained in Ref. [13] from a completely different viewpoint. In Ref. [13] the total pion multiplicity in the central rapidity region was estimated from the amount of entropy produced by the interacting parton system during the early stage of the nuclear collisions. This entropy was calculated within the parton cascade model from the partons' phase-space distributions as they evolve from the instant of collision through a pre-equilibrium stage to a thermalized quark-gluon plasma state. At this point no further entropy is produced on the parton level and the total produced entropy S in the central rapidity unit in central collisions was related to the pion multiplicity as

$$\frac{dS}{dy} = c^{(qg)} \left(\frac{dn^{(qg)}}{dy}\right)_{b=0} \approx \frac{c^{(\pi)}}{r} \left(\frac{dn^{(\pi)}}{dy}\right)_{b=0} , \tag{1}$$

where $dn^{(qg)}/dy$ and $dn^{(\pi)}/dy$ are the rapidity densities of quarks plus gluons, respectively pions and $b = 0$ indicates zero impact parameter. The statistical factors are $c^{(qg)} \simeq 4.0$, $c^{(\pi)} \simeq 3.6$ and $r = 0.7 \pm 0.2$ is the assumed ratio of the entropy density of a pion plasma to that of a quark-gluon plasma. Hence, the central pion multiplicity per unit rapidity in $Au + Au\,(b = 0)$ was estimated from the computed dS/dy according to

$$\left(\frac{dn^{(\pi)}}{dy}\right)_{b=0} \simeq (0.19 \pm 0.06)\,\frac{dS}{dy} , \tag{2}$$

resulting in $dn^{(\pi)}/dy \simeq 1900$ (3400) for $\sqrt{s} = 200$ A GeV ($\sqrt{s} = 6300$ A GeV). On the other hand, from Fig. 1 and with the result of Ref. [11] for the ratio of the charged to total hadron multiplicity $\langle n_{ch}\rangle/\langle n_{hadron}\rangle \simeq 0.6$, one gets a total hadron multiplicity of $\simeq 2000$ (4200) for $\sqrt{s} = 200$ A GeV ($\sqrt{s} = 6300$ A GeV) around zero rapidity. Roughly 75-85 % of these particles come out to be pions, which would imply $dn^{(\pi)}/dy \simeq$ 1500-1700 (3200-3500). Thus the charged particle multiplicities shown in Fig. 1 are quite consistent with the entropy production on the parton level. Additional entropy produced in the hadronization process is obviously neglegible compared to this large amount of entropy.

Turning to the transverse momentum distributions of charged particles shown in Fig. 2, one notices that the curves corresponding to the evolution schemes a) - e)

are hardly distinguishable in their shape (note that the curves have been multiplied by factors 10^k, $k = 0-4$, for better presentation). The slope is roughly the same for all five curves, at least for moderate $p_\perp \leq 3-4$ GeV. However, in the region $p_\perp \geq 6$ GeV the spectra appear to become slightly harder when comparing the curves from a) to e), in that this high $p_\perp$-domain becomes more populated. On the other hand, the comparison of the $p_\perp$-distributions for RHIC (Fig. 2 a) and LHC (Fig. 2 b) exhibits some interesting features: Aside from the already mentioned tripling of the total charged multiplicity, most prominent is the clear outgrowth of a power law tail for $p_\perp \geq 4$ GeV which is characteristic for the onset of QCD jet production. At RHIC ($\sqrt{s}$ = 200 A GeV) this high $p_\perp$ tail is just beginning to develop, but is almost invisible. At both energies, the low and moderate $p_\perp$-region ≤ 4 GeV is characterized by an approximate exponential distribution $\sim \exp(-p_\perp/p_0)$ with $p_0 \simeq 0.35$ GeV ($\sqrt{s}$ = 200 A GeV and $p_0 \simeq 0.39$ GeV ($\sqrt{s}$ = 6300 A GeV). The average $p_\perp$ however increases stronger [11], due to the significant $p_\perp$ contribution at LHC, namely from $\langle p_\perp \rangle \simeq 0.39$ GeV ($\sqrt{s}$ = 200 A GeV) to $\langle p_\perp \rangle \simeq 0.54$ GeV ($\sqrt{s}$ = 6300 A GeV) .

It is also instructive to compare the charged particle η- and $p_\perp$-spectra in $Au+Au$ collisions of Figs. 1 and 2 with the momentum distributions in $p+p$ collisions at the corresponding energies per nucleon. In $p+p$ ($p\bar{p}$) collisions the typical central rapidity densities are $\simeq 2.4$ for $\sqrt{s} = 200$ GeV and $\simeq 5.3$ for $\sqrt{s} = 6300$ GeV [13], whereas for $Au+Au$ at $b = 0$ fm the Fig. 1 (case e) shows central densities of $\simeq 1200$ ($\sqrt{s}$ = 200 A GeV) and $\simeq 2500$ ($\sqrt{s}$ = 6300 A GeV). Hence, even for the evolution scheme e) with the lowest multiplicities, one has $dn_{ch}^{AA}/d\eta|_{\eta=0} \simeq 2.4\ A\ dn_{ch}^{pp}/d\eta|_{\eta=0}$, i.e. significantly more more than twice the particle density per nucleon. However, for the total charged multiplicity per incident nucleon one gains only a factor ~ 1.5 from $p+p$ to $Au+Au$. This shows that the particle population is especially enhanced in the central rapidity region, as one intuitively would expect. Fig. 3 a emphasizes this enhancement by displaying the ratio of charged particle pseudorapidity distributions

$$R_{Au/p}(\eta) = \frac{dn_{ch}/d\eta(Au+Au)}{dn_{ch}/d\eta\,(p+p)} \tag{3}$$

over the whole η-range for the evolution scheme e). The multiplicity increase in $Au+Au$ collisions is particularly significant in the region $|\eta| \leq 2.5$ for $\sqrt{s} = 200$ A

GeV and $|\eta| \leq 6$ for $\sqrt{s} = 6300$ A GeV.

Confronting the charged particle $p_\perp$-spectra of $Au + Au$ collisions in Fig. 2 with the corresponding distributions in $p + \bar{p}$ collisions as done in Ref. [11], one observes a substantial suppression of high $p_\perp$ particle production in $Au + Au$ relative to $p + \bar{p}$. For example, at $\sqrt{s} = 200$ A GeV, the $p_\perp$-distribution in $Au + Au$ (Fig. 2 a) is of an exponential shape at least up to $p_\perp \simeq 5$ GeV, whereas the corresponding $p_\perp$-spectrum in $p + \bar{p}$ at $\sqrt{s} = 200$ GeV clearly exhibits a power law tail behaviour already for $p_\perp \geq 3$ GeV [11,13]. This feature is also reflected in Fig. 3 b where the ratio

$$R_{Au/p}(p_\perp) = \frac{dn_{ch}/dp_\perp^2\,(Au + Au)}{dn_{ch}/dp_\perp^2\,(p + p)} \tag{4}$$

of the inclusive $p_\perp$-spectrum of charged particles in central $Au + Au$ collisions to that of $p + p$ is plotted. One notices an enhancement in the hadron production of low and particularly of moderate $p_\perp$ particles which is peaked between ~ 1.5 and 3 GeV. On the other hand, there is obviously a strong suppression of particles at large $p_\perp$ which is mainly due to the increased energy loss especially of high $p_\perp$ partons in the range $p_\perp = 4-8$ GeV. This phenomenon is due to multiple scatterings and gluon radiations and has been studied also by Wang and Gyulassy [3] who find qualitatively the same behaviour. The observation of thermal shaped momentum distributions in $Au + Au$ in contrast to clearly non-thermal spectra in $p + p$ at the same energy per nucleon is of particular relevance when asking to which degree the final hadron distributions can reflect a thermalization of the partons in heavy ion collisions. In fact, due to the extended time scale of a heavy ion reaction and the dense phase-space population of partons in the central region, the energy and momentum brought into the collision can quickly get distributed through frequent multiple interactions among the quanta [7,14]. As a consequence, the final charged particle spectra exhibit a resemblance with thermal distributions which is not noticable in dilute and small sized systems as in hadron-hadron collisions.

Finally I would like to comment on the possibility to experimentally disentangle the different phenomena of nuclear shadowing, parton fusion and absorption, the Landau-Pomeranchuk effect and soft gluon interference. It has already been emphasized in Ref. [3] that $A + A$ data alone would not be sufficient to separate

the various effects, but $p + A$ reactions must be studied too at the same energy. As mentioned before, soft gluon interference is a general QCD property of the partons and it presumably does not depend on the reaction considered. Hence, the suppression of hadron production in the small rapidity region associated with soft gluon interference should factor out in the ratio (3) and the relative enhancement of $dn_{ch}/d\eta$ in $A + A$ relative to $p + p$ (Fig. 3 a) should be independent of this effect. On the other hand, in $p + A$ collisions, the density of comoving hadrons is, compared to $A + A$ reactions, rather low. Therefore parton fusion and absorption as well as the Landau-Pomeranchuk effect should play a minor role in $p + A$, because both these effects are connected to a dense phase-space population of partons. In view of these considerations I would like to propose to systematically study *both* the two ratios

$$\begin{aligned} \rho^{AB}(\eta) &= \frac{dn_{ch}/d\eta(A+B)}{dn_{ch}/d\eta(p+p)} \\ \rho^{AB}(p_\perp) &= \frac{dn_{ch}/dp_\perp^2(A+B)}{dn_{ch}/dp_\perp^2(p+p)} \end{aligned} \tag{5}$$

for the charged particle spectra in $p + A$ *and* $A + A$ collisions. From the measurement of $\rho^{pA}(p_\perp)$ the amount of nuclear shadowing could be determined by comparing it to $\rho^{AA}(p_\perp)$. In addition, here it could be tested if the effects of soft gluon interference are indeed independent of the reaction. Then, by subtracting the contribution of shadowing in $A + A$ collisions, the suppression of hadron production around $\eta \approx 0$ due to enhanced parton fusion and absorption and the Landau-Pomeranchuk effect could be isolated by analyzing $\rho^{pA}(\eta)$ and $\rho^{AA}(\eta)$. Moreover, with the magnitude of shadowing determined, the measurement of $\rho^{pA}(p_\perp)$ would allow to separate the effect of the suppression of moderate $p_\perp$ hadrons in $A + A$ collisions (Fig. 3 b), which is due to the increasing role of multiple parton interactions and parton cascading.

In conclusion, calculations for central $Au + Au$ collisions at beam energies $\sqrt{s} =$ 200 A GeV and $\sqrt{s} =$ 6300 A GeV with the parton cascade / cluster hadronizations model of Ref. [11] shed some light on the important role of a number of nuclear and medium effects associated with the space-time evolution of partons in ultra-relativistic heavy ion collisions. In particular, it was illustrated by analyzing

the model results for the momentum distributions of charged hadrons that nuclear shadowing, the Landau-Pomeranchuk effect, parton fusions and absorptions, and the destructive interference of soft gluons in the parton cascades lead to hadron spectra drastically different from the results of the naive calculation which neglects these effects. The most prominent feature is the strong reduction of the charged hadron yield by more than a factor of 3 in the central rapidity region. The predicted charged multiplicities in the central rapidity unit are $\simeq 1200$ for $\sqrt{s} = 200$ A GeV and $\simeq 2500$ for $\sqrt{s} = 6300$ A GeV. The ratio of charged to total multiplicity comes out to be $\simeq 0.6$. Furthermore, in comparison with $p + p$ collisions at the same energies the model predicts a factor of about 2.5 per incident nucleon in the increase for the total multiplicities of particles produced in the central region. Also, the $p_\perp$-spectra of $Au + Au$ relative to $p + p$ collisions show a considerable suppression of hadron production for $p_\perp \geq 4$ GeV, due to the mentioned effects. In contrast to $p + p$ the hadronic momentum distributions in $Au + Au$ exhibit a resemblance with thermal spectra which indicates the reflection of thermalization properties of the partons during the nuclear reactions. This may offer the possibility to learn about a quark gluon plasma phase-transition from analyzing the hadronic spectra of ultra-relativistic heavy ion collisions.

ACKNOWLEDGEMENTS

I would like to express very special thanks to J. Kapusta for his encouraging support in every respect. Also I thank B. Müller for his open ears and X. N. Wang for stimulating discussions. The numerical computations were performed on the two *Cray* computers of the Minnesota Supercomputer Institute and on a *Silicon Graphics* computer at Duke University. This work was supported by the U.S. Department of Energy under Contract No. DOE/DE-FG02-87ER-40328.

REFERENCES

[1] See e.g. B. Müller, *The Physics of the Quark Gluon PLasma*, Lecture Notes in Physics 225 (Springer, Heidelberg 1985); L. McLerran, *Rev. Mod. Phys.* **58** (1986), 1021; *Quark Gluon Plasma*, edited by R. C. Hwa (World Scientific, Singapore 1990); *Quark Matter '91, Proceedings of the Ninth Inter-*

national Conference on Ultrarelativistic Nucleus-Nucleus Collisions, Gatlinburg, 1991, To appear in *Nucl. Phys.* **A**.

[2] X. N. Wang and M. Gyulassy, *Phys. Rev.* **D44** (1991), 3501.

[3] X. N. Wang and M. Gyulassy, *Phys. Rev. Lett.* **68** (1992), 1480.

[4] L. L. Frankfurt and M. I. Strikman, *Phys. Rep.* **160** (1988),235.

[5] European Muon Collaboration, J. Ashman et al., *Phys. Lett.* **B202** (1988), 603; European Muon Collaboration, M. Arneodo et al., *Phys. Lett.* **B211** (1988), 493.

[6] F. E. Close, J. Qiu and R. G. Roberts, *Phys. Rev.* **D 40** (1989), 2820; A. H. Mueller, *Nucl. Phys.* **B335** (1990), 115.

[7] K. Geiger, *Thermalization in Ultrarelativistic Nuclear Collisions - I. Parton Kinetics and Quark Gluon Plasma Formation*, University of Minnesota preprint, Minneapolis, 1992 (submitted to Phys. Rev. D).

[8] L. D. Landau and I. Ya. Pomeranchuk, *Dokl. Akad. Nauk SSSR* **92** (1953), 535, 735.

[9] A. Bassetto, M. Ciafaloni and G. Marchesini, *Phys. Rep.* **100** (1983), 203.

[10] K. Geiger and B. Müller, *Nucl. Phys.* **B369** (1992), 600.

[11] K. Geiger, *Particle Production in Ultra-relativistic Nuclear Collisions - A Parton Cascade / Cluster Hadronization Model*, University of Minnesota preprint, Minneapolis, 1992 (submitted to Phys. Rev. D).

[12] G. Marchesini and B. R. Webber, *Nucl. Phys.* **B238** (1984), 1; B. R. Webber, *Nucl. Phys.* **B238** (1984), 492; G. Marchesini and B. R. Webber, *Nucl. Phys.* **B310** (1988), 461.

[13] X. N. Wang and M. Gyulassy, *Phys. Rev.* **D45** (1992), 844.

[14] K. Geiger, *Thermalization in Ultrarelativistic Nuclear Collisions - II. Entropy Production and Energy densities at RHIC and LHC*, University of Minnesota preprint, Minneapolis, 1992 (submitted to Phys. Rev. D).

FIGURE CAPTIONS

Fig. 1: The model predictions (solid histogram) for the pseudorapidity distributions of charged particles in central $Au + Au$ collisions at $\sqrt{s} = 200$ A GeV (left) and $\sqrt{s} = 6300$ A GeV (right). The various histograms show the characteristics of the space-time evolution schemes defined in the text: a) 'naive' evolution (dotted), b) nuclear shadowing (long dashed), c) parton fusion and absorption (dashed dotted), d) Landau-Pomeranchuk effect (short dashed), and e) soft gluon interference (solid). Note that case e) is the full calculation including all these effects.

Fig. 2: The model predictions (solid histogram) for the transverse momentum distributions of charged particles in central $Au + Au$ collisions at $\sqrt{s} = 200$ A GeV (left) and $\sqrt{s} = 6300$ A GeV (right). As in Fig. 1 the different histograms refer to the space-time evolution schemes a) - e) defined in the text (for better presentation the distributions have been multiplied by powers of 10): a) 'naive' evolution (dotted), b) nuclear shadowing (long dashed), c) parton fusion and absorption (dashed dotted), d) Landau-Pomeranchuk effect (short dashed), and e) soft gluon interference (solid). Note that case e) is the full calculation including all these effects.

Fig. 3: The model results for the ratio of the inclusive charged hadron spectra of central $Au + Au$ collisions to those of $p + p$ for $\sqrt{s} = 200$ A GeV (dashed histogram) and $\sqrt{s} = 6300$ A GeV (solid histogram). Both the ratio of pseudorapidity distributions (left) and the one of the transverse momentum distributions (right) were calculated with the space-time evolution scheme e) defined in the text and include the phenomena of nuclear shadowing, parton fusion and absorption, the Landau-Pomeranchuk effect and soft gluon interference.

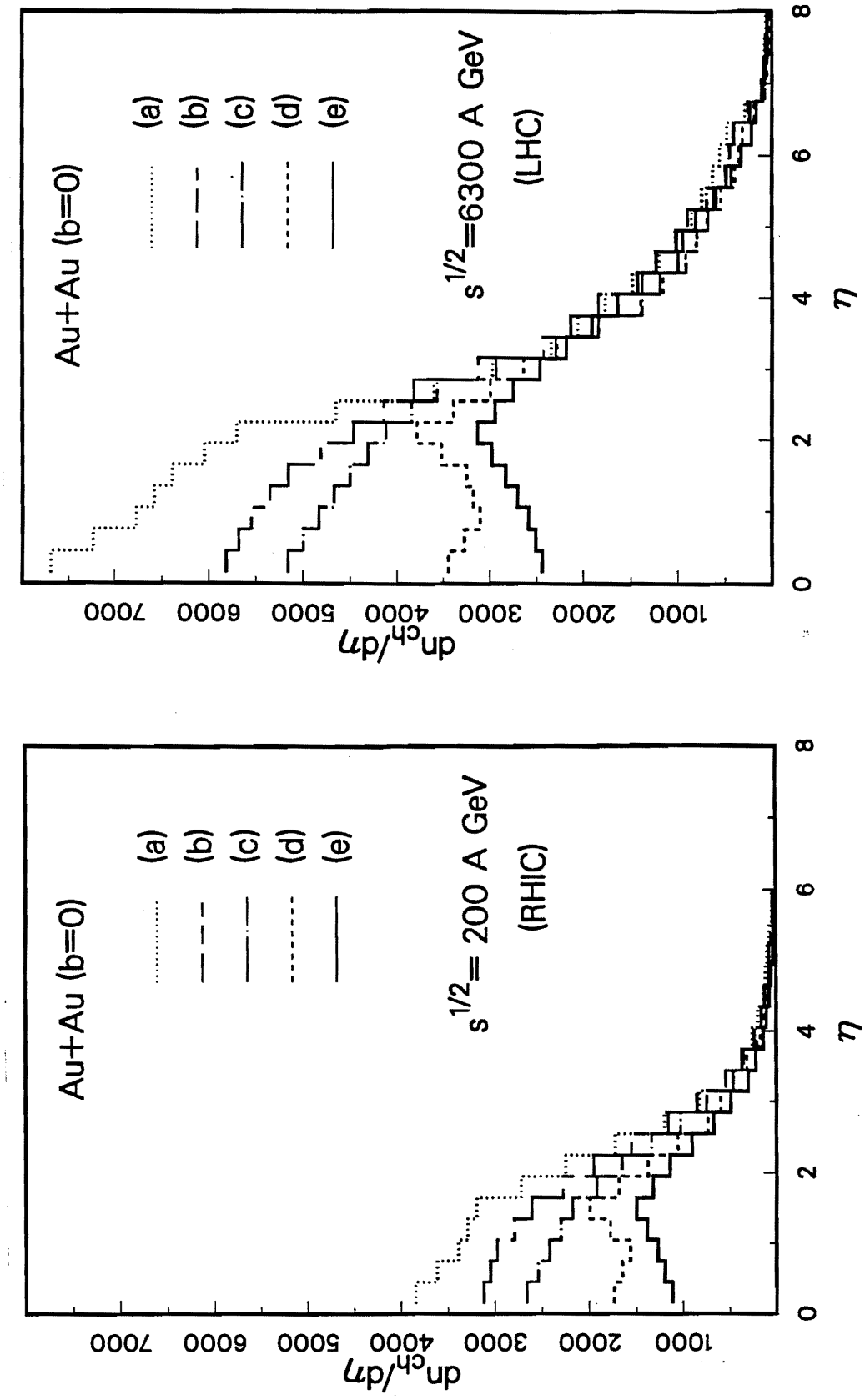
Au+Au (b=0)
(a)
(b)
(c)
(d)
(e)
s^1/2= 200 A GeV
(RHIC)
dn_ch/dη
η
Au+Au (b=0)
(a)
(b)
(c)
(d)
(e)
s^1/2=6300 A GeV
(LHC)
dn_ch/dη
η

Figure 1

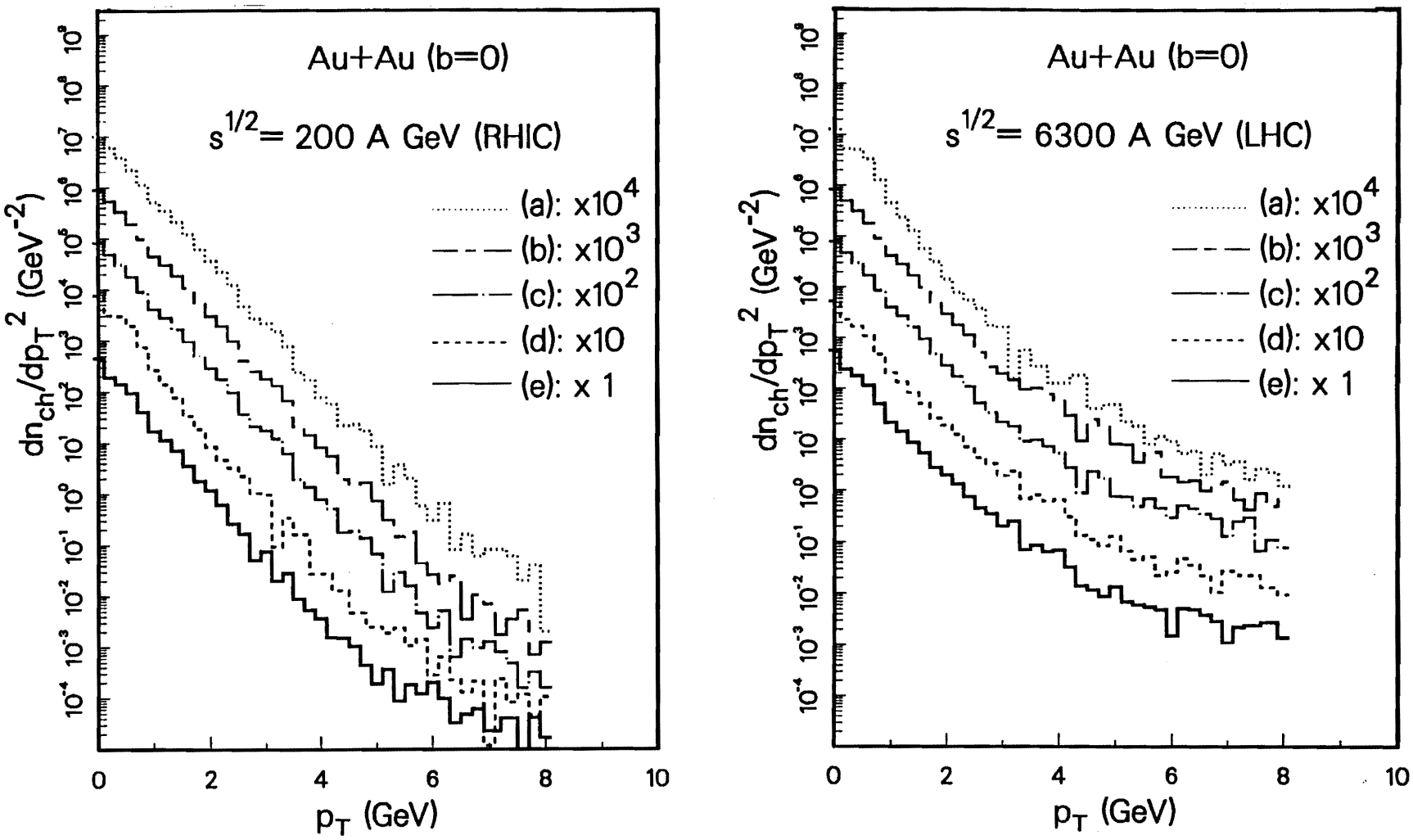
Au+Au (b=0)
$s^{1/2}$= 200 A GeV (RHIC)
(a): x10^4
(b): x10^3
(c): x10^2
(d): x10
(e): x 1
dn_{ch}/dp_T^2 (GeV^{-2})
p_T (GeV)
Au+Au (b=0)
$s^{1/2}$= 6300 A GeV (LHC)
(a): x10^4
(b): x10^3
(c): x10^2
(d): x10
(e): x 1
dn_{ch}/dp_T^2 (GeV^{-2})
p_T (GeV)

Figure 2

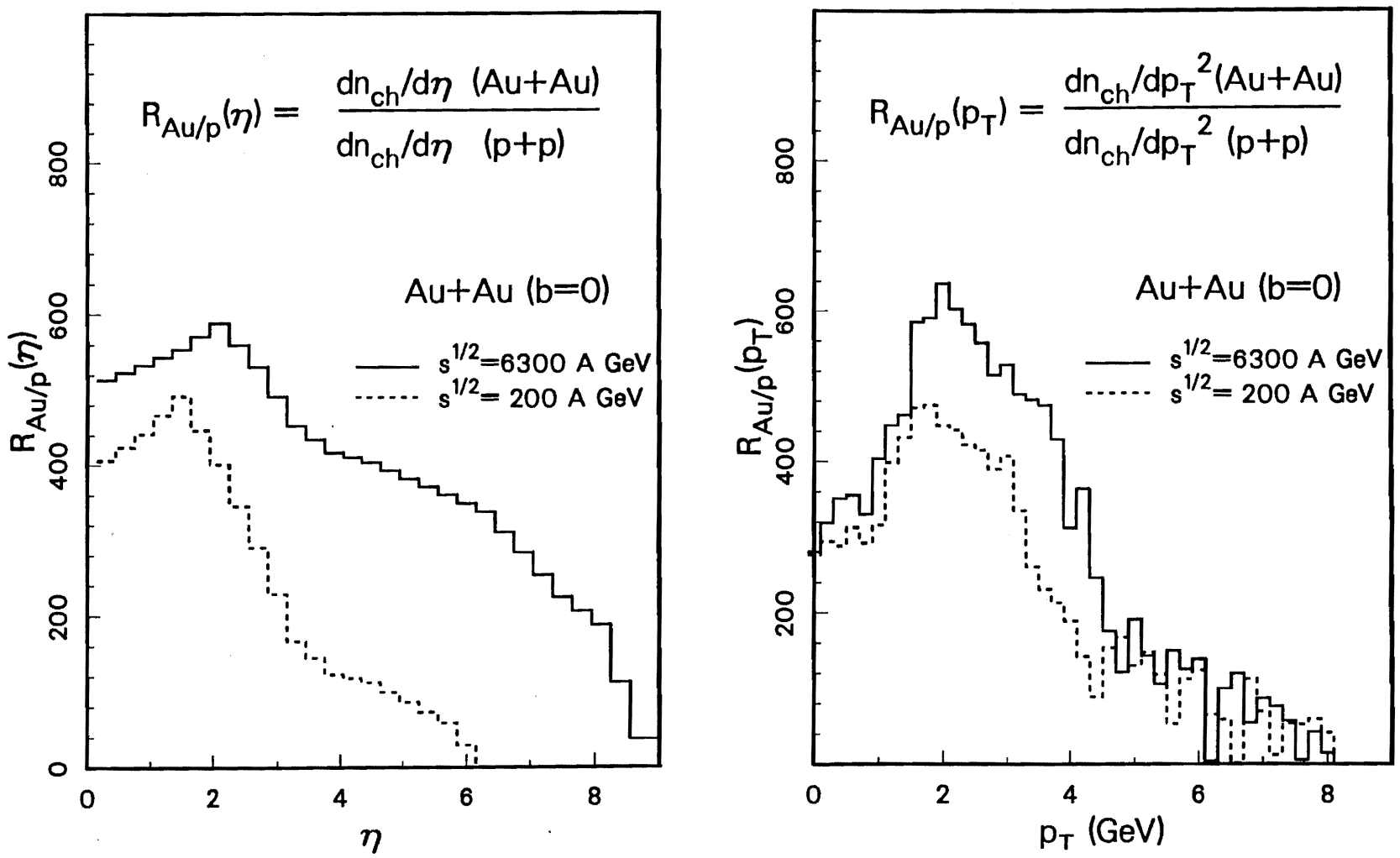
$R_{Au/p}(\eta) = \frac{dn_{ch}/d\eta \ (Au+Au)}{dn_{ch}/d\eta \ (p+p)}$
Au+Au (b=0)
$s^{1/2}$=6300 A GeV
$s^{1/2}$= 200 A GeV
$R_{Au/p}(\eta)$
η
$R_{Au/p}(p_T) = \frac{dn_{ch}/dp_T^2 (Au+Au)}{dn_{ch}/dp_T^2 \ (p+p)}$
Au+Au (b=0)
$s^{1/2}$=6300 A GeV
$s^{1/2}$= 200 A GeV
$R_{Au/p}(p_T)$
p_T (GeV)

Figure 3